



A finite-element approach for the analysis of pin-bearing failure of composite laminates

Michele Marino

*Università degli Studi di Roma "Tor Vergata", Department of Civil Engineering and Computer Science Engineering (DICII),
00133 Rome, Italy
m.marino@ing.uniroma2.it*

Francesca Nerilli

*Unicusano - Università degli Studi Niccolò Cusano - Telematica Roma, 00166 Rome, Italy
francesca.nerilli@unicusano.it*

Giuseppe Vairo

*Università degli Studi di Roma "Tor Vergata", Department of Civil Engineering and Computer Science Engineering (DICII),
00133 Rome, Italy
vairo@ing.uniroma2.it*

ABSTRACT. In this paper, a numerical home-made finite element model for the failure analysis of bolted joints between fiber-reinforced composite laminates is presented. The model is based on an incremental displacement-based approach, it is hinged on the laminate theory and on a progressive material degradation governed by the failure of composite constituents. The model has been applied to a pin-plate system comprising a mono-directional fiber-reinforced laminated plate, and numerical results in terms of the bearing failure load have been successfully compared with available experimental data. Aim of this paper is to evaluate the effectiveness of Rotem's and Huang's failure criteria in predicting the pin-bearing failure of bolted joints. The selected criteria act at different material scale: the former operating at the laminate level, while the latter at the constituent's scale. Proposed results seems to suggest that failure criteria accounting for micro-structural stress-strain localization mechanisms (for instance, Huang's criterion) give a more accurate estimate in terms of pin-bearing failure load.

KEYWORDS. FRP composite laminates; Bolted joints; Progressive damage; Pin-bearing failure.

INTRODUCTION

The increased use of fiber reinforced polymer (FRP) composite materials in civil structural applications, and its corresponding advantages, such as, high specific strength and stiffness, and high corrosion resistance, requires the development of advanced design methods. Despite the fact that this type of structural elements have many advantages and potentials, structural joints remain an unavoidable need. Joints represent structural discontinuities

associated with stress localization: for many practical applications, structural joining (both adhesive and bolted) could represent a gap for the structural behavior because of their failure mode.

Failure modes of bolted joints in laminated composite plates under tensile loads usually occur in four basic modes: cleavage, net-tension, shear-out and bearing modes. In detail, local bearing failure modes are characterized by a local laminate compressive failure caused by the bolt diameter which tends to crush the composite material. Pin-bearing failure mode of bolted FRP joints, locally associated with matrix cracks, is an important design problem that has attracted the interest of the international scientific community, as confirmed by the great number of researches carried out in the last years [1–10]. Results of these studies have highlighted that both geometric (e.g., bolt diameter, plate width and thickness, end distance) and material properties (e.g., fiber inclination angle, matrix type and fiber nature, stacking sequence) highly affect the strength and the failure mode of FRP-based jointed elements. Accordingly, a computational model able to give parametric indications on the mechanical performance of bolted FRP joints, as well as able to predict their failure mechanisms, would be a powerful and useful design tool for both civil and mechanical advanced applications.

Aim of this paper is to develop a numerical model based on a non-linear finite-element formulation for the analysis of the progressive damaging and the failure modes in bolted joints between fiber-reinforced composite laminates. The numerical formulation, applied to a pin-plate system, is based on a plane-stress bidimensional model and on an incremental displacement-based approach driven by the pin position. Neglecting friction, the unilateral contact at the pin-plate interface has been treated through a surface-to-surface penalty method. In order to describe the damage evolution, the model implements two failure criteria available in the literature (by Rotem [13] and Huang [15]), involving different stress-strain measures at different material scales.

The obtained results have been successfully compared with the experimental data in [10], allowing to show soundness and accuracy of the proposed formulation, as well as to highlight the effectiveness and/or possible limitations of the considered failure criteria.

THEORETICAL BACKGROUND

FRP composite laminates are made of layers (plies) bonded together to form a plate-like structural element. Each ply consists in unidirectional continuous fibers embedded in a polymeric matrix, with a preferred fiber direction. Accordingly, each composite ply exhibits a global constitutive response characterized by a transversely isotropic symmetry, with the isotropic plane orthogonal to the fiber direction.

In the following, as a notation rule, for each layer the subscript \mathcal{A} denotes the direction parallel to the fibers, T the transverse-to-the-fibers direction, and symbols +/- discriminate strength material properties in traction and compression, respectively. Furthermore the generic constituent is indicated by the subscript c ($c = f$ for fibers and $c = m$ for matrix).

The fiber's undamaged material is assumed to be linearly elastic, with symmetry plane orthogonal to the fiber's axis (with engineering constants E_f^A , E_f^T , G_f^{AT} , ν_f^{AT} , ν_f^T), and the matrix's undamaged material is isotropic linearly elastic (with engineering constants E_m and ν_m). FRP layers and laminated plates are assumed to be planar and characterized by small thicknesses. Accordingly, a plane-stress condition is assumed in the following.

The ability to predict initiation and growth of damage in bolted FRP joints can only be offered by progressive damage modeling techniques. Failure analysis of laminate composites are made up of three main ingredients: stress analysis through homogenization theories, failure analysis by means of strength criteria for composite layers, and a material degradation law for describing the failure occurrence in composite constituents.

Stress analysis

In order to determine the mechanical properties of the laminate a refined homogenization procedure, that takes into account localization mechanisms, has been used. Accordingly, in agreement with the Huang's indications, the *Bridging Model* [14] is herein employed.

Addressing a single composite layer with mono-directional fiber direction, the 6x6 equivalent homogeneous compliance matrix $[S] = [s_{ij}]$, expressed in a local coordinate system (\mathcal{A}, T, T) , results in:

$$[S] = \left\{ \nu_f [S^f] + \nu_m [S^m] [A] \right\} \left\{ \nu_f [I] + \nu_m [A] \right\}^{-1} \quad (1)$$



where v_f is the fiber volume fraction, $v_m = 1 - v_f$, $[I]$ is the identity matrix, $[S^c] = [s_{ij}^c]$ the compliance matrix for the constituent c , and $[A] = [a_{ij}]$ is the bridging matrix. In the case of a plane-stress state $[S]$, $[S^c]$ and $[A]$ reduce to 3x3 matrices, with $[A]$ defined component-wise by [14]:

$$a_{11} = \frac{E_m}{E_f^A}, \quad a_{22} = 0.5 \left(1 + \frac{E_m}{E_f^T} \right), \quad a_{33} = 0.5 \left(1 + \frac{G_m}{G_f^{AT}} \right), \quad a_{21} = a_{31} = a_{32} = 0 \quad (2)$$

$$a_{12} = \frac{(s_{12}^f - s_{12}^m)(a_{11} - a_{22})}{s_{11}^f - s_{11}^m}, \quad a_{13} = \frac{d_2 \beta_{11} - d_1 \beta_{21}}{\beta_{11} \beta_{22} - \beta_{12} \beta_{21}}, \quad a_{23} = \frac{d_1 \beta_{22} - d_2 \beta_{12}}{\beta_{11} \beta_{22} - \beta_{12} \beta_{21}}, \quad (3)$$

where

$$d_1 = s_{13}^m (a_{11} - a_{33}), \quad d_2 = s_{23}^m (v_f + v_m a_{11})(a_{22} - a_{33}) + s_{13}^m (v_f + v_m a_{33})(a_{12}) \quad (4)$$

$$\beta_{11} = s_{12}^m - s_{12}^f, \quad \beta_{12} = s_{11}^m - s_{11}^f, \quad \beta_{22} = (v_f + v_m a_{22})(s_{12}^m - s_{12}^f) \quad (5)$$

$$\beta_{21} = (v_m)(s_{12}^f - s_{12}^m)a_{12} - (v_f + v_m a_{11})(s_{22}^f - s_{22}^m) \quad (6)$$

Referring to composite laminated plates comprising mono-directional fiber-reinforced layers, stress analysis is conducted by employing the classical laminate theory [12], where the compliance matrix $[S]_k$ of each k -th composite layer is obtained from Eq. (1), and it is suitably expressed by passing from the local coordinate system (aligned with the fiber direction) to a global reference one.

When necessary, a local stress measure for each layer's constituent can be recovered starting from the homogenized stress field within the layer and by considering as localization matrices $[B]$ and $[A][B]$ for fiber and matrix, respectively, where the 3x3 matrix $[A]$ is defined in Eqs. (2-6), and the 3x3 matrix $[B]$ is defined (in components) as:

$$b_{11} = (v_f + v_m a_{22})(v_f + v_m a_{33}) / \rho, \quad b_{12} = -(v_m a_{12})(v_f + v_m a_{33}) / \rho, \quad b_{21} = b_{31} = b_{32} = 0 \quad (8)$$

$$b_{13} = [(v_m a_{12})(v_m a_{23}) - (v_f + v_m a_{22})(v_m a_{13})] / \rho, \quad b_{22} = (v_f + v_m a_{11})(v_f + v_m a_{33}) / \rho \quad (9)$$

$$b_{23} = -(v_m a_{23})(v_f + v_m a_{11}) / \rho, \quad b_{33} = (v_f + v_m a_{22})(v_f v_m a_{11}) / \rho \quad (10)$$

where $\rho = (v_f + v_m a_{11})(v_f + v_m a_{22})(v_f + v_m a_{33})$. In detail, referring to an incremental approach, and denoting with $d\bar{\sigma}_k$ the increment of the homogenized stress vector within the k -th layer, the corresponding stress increments in fiber and matrix result in:

$$d\bar{\sigma}_f = [B]d\bar{\sigma}_k, \quad d\bar{\sigma}_m = [A][B]d\bar{\sigma}_k \quad (11)$$

Failure analysis

Failure analysis has been based on local criteria. In detail, two approaches differently accounting for micro-mechanical features have been employed to predict degradation of the constituents' material properties.

The first criterion herein considered, provided by Rotem [13], operates on the stress state $\bar{\sigma}_k$ in the k -th laminate layer, whose increment results from $d\bar{\sigma}_k = [S]_k^{-1}d\bar{\epsilon}$, where $[S]_k$ is computed by Eq. (1) and where $d\bar{\epsilon}$ is the homogenized strain increment in the laminate. This latter is obtained as the solution of the incremental problem and it is assumed to be constant along the laminate thickness. This criterion is based on the basic assumptions that: a) the failure onset is a localized phenomenon, b) only in-plane stresses are effective (that is, interlaminar stresses do not cause failure), c) the matrix material is weaker and softer than the fibers. In agreement with this approach, it is also assumed that micro-buckling does not occur. On the basis of these assumptions the failure criterion actually combines two separate criteria, a failure criterion along the fibers direction and a failure criterion along the transversal-to-fibers direction. The fibers, being



stiffer and stronger than the matrix, can only fail due to loads acting in their axial direction. By omitting the subscript k discriminating different layers and addressing a single FRP layer, transversal failure occurs when

$$\left(\frac{\bar{\sigma}_T}{S_T^{+/-}}\right)^2 + \left(\frac{\bar{\sigma}_{AT}}{S_{AT}}\right)^2 \geq 1, \tag{12}$$

where $S_T^{+/-}$ is the laminate strength (respectively in tension and compression) in the transverse-to-the-fibers direction, while S_{AT} is the shear laminate strength. On the other hand, the fiber failure criterion is expressed by the following relationships:

$$\bar{\sigma}_A \geq S_A^+, \quad \bar{\sigma}_A \leq -S_A^- \tag{13}$$

where S_A^+ and S_A^- are the laminate strengths (respectively in tension and compression) along the fibers direction. The second criterion, provided by Huang [15], operates on the stress states in fibers ($\bar{\sigma}_f$) and matrix ($\bar{\sigma}_m$), different in each layer and computed starting from the layer stress state $\bar{\sigma}_k$ by employing Eq. (11). Accordingly, it prescribes tensile failure for the constituent c if

$$\sigma_{eq,c} \geq S_c^+, \tag{14}$$

where S_c^+ is the tensile strength for the constituent c , and

$$\sigma_{eq,c} = \begin{cases} \sigma_c^{(1)} & \text{when } \sigma_c^{(2)} \leq 0 \\ \left[\left(\sigma_c^{(1)} \right)^{q_c} + \left(\sigma_c^{(2)} \right)^{q_c} \right]^{\frac{1}{q_c}} & \text{when } \sigma_c^{(2)} \geq 0, 1 < q_c \leq \infty \end{cases} \tag{15}$$

q_c being a power index accounting for the effects of a biaxial stress state on the bearing capacity, and $\sigma_c^{(1)}$, $\sigma_c^{(2)}$ are the first (maximum) and the second (minimum) principal stresses in the constituent c . Furthermore, a compressive failure of the constituent is assumed to occur if

$$\sigma_c^{(2)} \leq -S_c^- \tag{16}$$

where S_c^- is the compressive strength for the constituent c .

Material property degradation

In this study, a simple degradation rule is employed by assuming that a damaged constituent reduces its elastic moduli by the factor $\eta > 1$. When the Rotem failure criterion is used, the overall laminate stiffness matrix is locally degraded, while, by using the Huang failure criterion, the elastic moduli of fibers or matrix are locally degraded, depending on the damaged component.

PROBLEM STATEMENT

The effectiveness of the proposed progressive damage model is verified by addressing as a benchmark the experimental study by Ascione et al. [10], carried out on a pin-plate system comprising a glass fiber reinforced polymer (GFRP) laminate with epoxy matrix. This experimental investigation aimed to analyze the influence of the fiber-to-load inclination angle, referred to as α , on the bearing failure load associated to the action of a steel pin (see Fig. 1). In particular the experiments in [10] considered three types of laminates, different in the stacking sequences of the plies. Herein reference is made to the laminate type denoted in [10] as *Laminate 1*, consisting in a square-shaped plate (500 mm wide) and comprising eight equally-oriented plies of Continuous Strand Mat GFRP material placed between two plies of Chopped Strand Mat (CSM), resulting in the plying sequence $[CSM/0_4]_s$. The plate was tighten by two steel plates 500 mm wide and 50 mm thick, with a central circular hole of 300 mm in diameter (see Fig. 1). The higher stiffness of the

steel plates with respect to the GFRP laminate allows to regard the testing system as statically equivalent to the central circular region undergoing perfectly fixed conditions on its boundary. At the center of that circular region of the laminated plate a circular hole with diameter $D = 20$ mm was considered, wherein a steel pin with diameter $d \leq D$ was inserted and acted upon by a testing load parallel to the laminated plate. Different values of d were considered in [10]. In the present study, reference has been made to experimental results relevant only to the case $d = D$. The fiber volume fraction for the laminated plate was equal to about 60%, and the plate thickness was equal to 10 mm: 1 mm for each CSM layer and 1 mm for each mono-directional layer. This type of laminate is identified in the literature as “mono-directional”, despite the presence of two CSM layers, which can be treated as almost isotropic [11]. Bearing failure load, defined as the peak in the pin load-displacement curve, has been obtained in [10] for $\alpha \in [0^\circ, 90^\circ]$, observing that it is highly sensitive with α .

NUMERICAL MODEL

In order to simulate the failure mode and to evaluate the pin-bearing load of the laminated plate tested in [10], a 2D numerical model has been developed. A Matlab home-made code has been employed for the numerical analysis, with the use of the libraries encoded in the commercial solver Comsol Multiphysics for the finite-element computations and for managing the non-linear contact problem.

The plate external boundary undergoes fully restrained conditions (see Fig. 2), in agreement with the experimental setting used in [10]. Due to the small thickness-to-side ratio of the plate and since the symmetric plying sequence of the laminate, the plane stress assumption has been enforced. Neglecting friction, the unilateral contact at the pin-plate interface has been treated through a surface-to-surface penalty method.

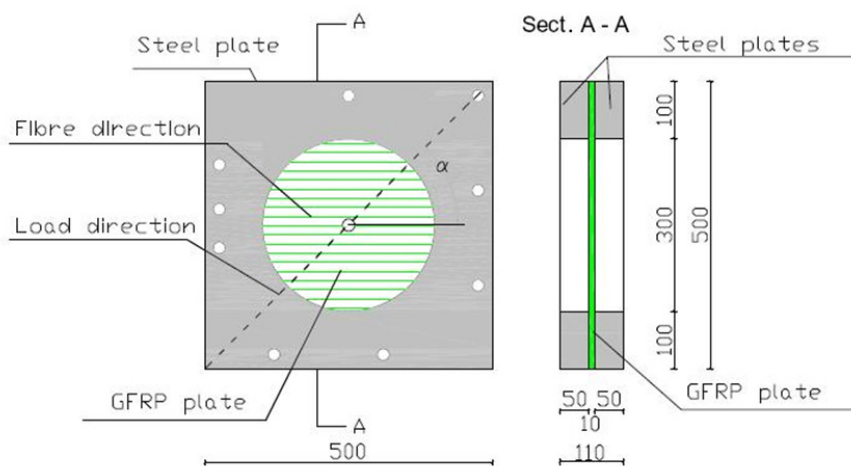


Figure 1: GFRP composite sample addressed in [10] (dimensions in mm).

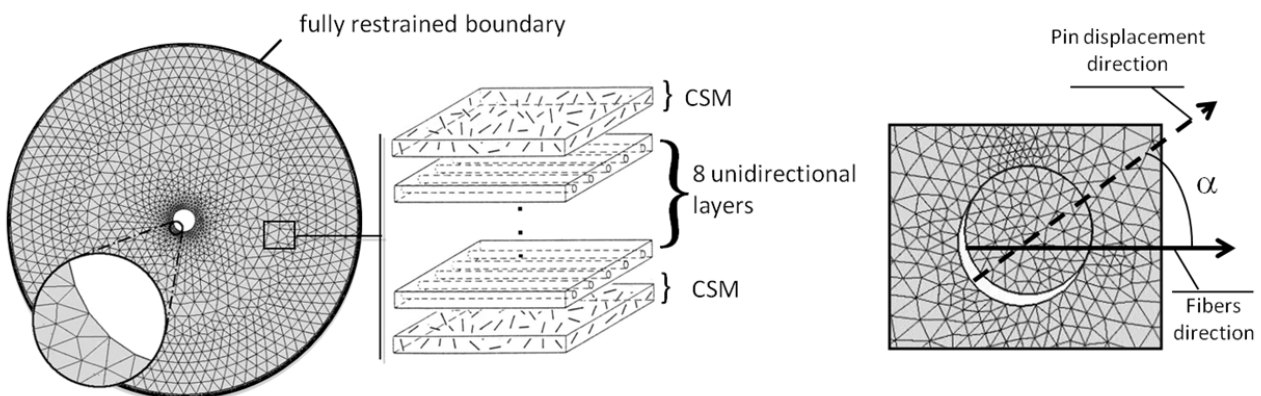


Figure 2: Mesh details, loading conditions and laminate plying pattern employed for numerical simulations (on the left, pin is not shown).



The finite-element mesh has been obtained by triangular elements, based on a pure displacement formulation with quadratic displacement shape functions. Resulting from a numerical convergence analysis, computational mesh consisted in about 150.000 elements. In order to deal with convergence issues related to contact non-linearities, a mesh refinement around the pin-plate interface, characterized by an average mesh size of about $0.1D$, has been employed.

As reported in Tab. 1, stiffness properties for fiber and matrix constituents are taken from [10]. In Tab. 1, strength properties for composite constituents (needed for Huang's criterion and chose from [10]) are also reported. For the sake of simplicity, proposed results are based on the assumption of symmetric tensile/compressive strength of all constituents. Moreover, the undamaged CSM is treated as an isotropic linearly elastic material (with engineering constants E_{CSM} and ν_{CSM}) whose damage is predicted through the Von Mises criterion (with strengths $S_{CSM}^{+/-}$), [17]. Finally, the pin is assumed to comprise an isotropic linearly elastic material (with constants E_p and ν_p), and no damage is modeled for it. In Tab. 2, the mechanical strength of the GFRP Laminate (needed for the Rotem's criterion), experimentally determined in [9], are also provided.

Fibers:	$S_f^+ = S_f^-$	2.5 GPa	Matrix:	$S_m^+ = S_m^-$	26 MPa
	$E_f^A = E_f^T$	50 GPa		E_m	1.4 GPa
	$\nu_f^A = \nu_f^T$	0.18	Pin:	E_p	210 GPa
CSM:	$S_{CSM}^+ = S_{CSM}^-$	250 MPa	Others:	η	100
	E_{CSM}	12.41 GPa		q (Huang)	5
	ν_{CSM}	0.4		N	20
				ν_m	0.4
				ν_p	0.3

Table 1: Undamaged material properties of the layer constituents, CSM, pin and other model parameters [10,14,17,16].

Laminate:	S_A^+	222 MPa
	S_A^-	201 MPa
	S_T^+	71 MPa
	S_T^-	81 MPa
	S_{AT}	128.17 MPa

Table 2: Mechanical strength of the GFRP laminate [9].

The numerical model is based on an incremental displacement approach driven by the pin position. The plate damage has been evaluated with an iterative numerical procedure, summarized in the flowchart depicted in Fig. 3. In detail, after the geometric modeling, equivalent homogenized material properties are locally assigned for each element on the basis of the laminate theory [12] and by adopting the afore-mentioned homogenization technique. At each incremental step, FEM-based solution allows to compute the increment of the strain field $d\bar{\epsilon}$ representing an average measure along the laminate thickness for the overall laminate. By involving the constitutive relationships, the incremental field $d\bar{\epsilon}$ is used to compute the increment of the average stress field for the laminate, as well as (if necessary) the increment of the stress field in each layer and in its constituents. Accordingly, addressing the actual stress field, obtained by superimposing stress increments, a given failure criterion is employed in order to verify possible damage occurrence. If failure conditions are not detected for undamaged constituents, the geometry of the pin-plate system is updated, fibers packaging is updated on the basis of the computed strain field increment, and the value of pin displacement is increased to perform the analysis of a new incremental step. Otherwise, if damage locally occurs, material properties are locally altered by employing the degradation law previously introduced. In order to check if progressive material degradation occurs at that step, the actual incremental step is repeated with the same geometry and under the same boundary conditions until further material failure is no longer detected in the overall computational domain. If this iterative procedure is repeated for a number N of occurrences (see Tab. 1), the global failure condition is assumed to be reached and the numerical integral of the



distributed reaction force at the external boundary of the plate is considered as a measure of the corresponding failure load.

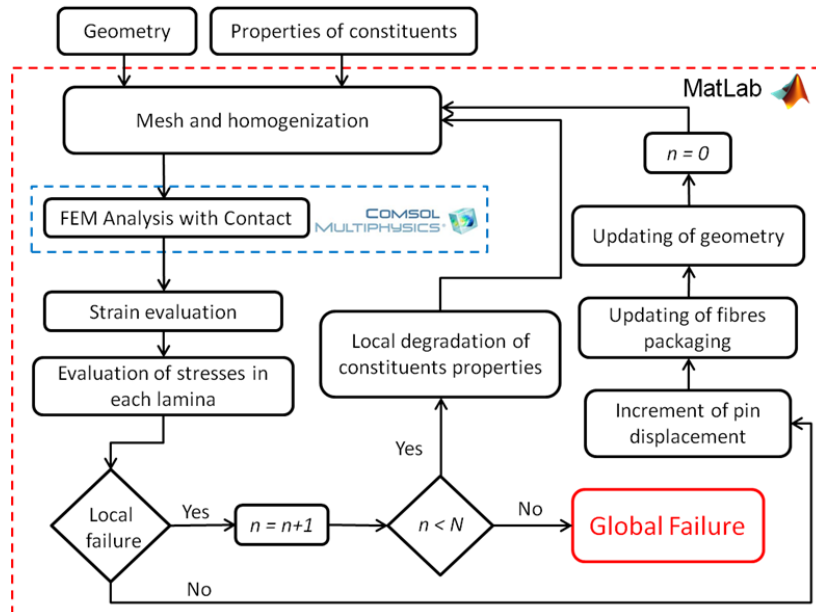


Figure 3: Flowchart of the incremental numerical procedure implemented in this study.

RESULTS

Rotem and Huang failure criteria are compared in Fig. 4 with experimental data proposed in [10]. Both criteria describe the qualitative trend experimentally tested, but while the Huang's criterion provides a more accurate quantitative prediction of the failure load, the Rotem's one widely under-estimates (resp., over-estimates) the value of the ultimate load for $\alpha = 90^\circ$ (resp., $\alpha = 0^\circ$). This result is mainly induced by the simplifying assumption adopted by Rotem that fibers only are responsible for longitudinal failure, while matrix only for transverse and shear failure. When fiber direction and pin displacement direction are parallel ($\alpha = 0^\circ$) the highest components of the average stress field in the plate are along the fiber direction and are associated by the Rotem's criterion entirely to the strength $S_A^{+/-}$. Accordingly, since the fibers' high longitudinal strength, the failure condition occurs at higher loads than the experimental evidence. In fact, damage, which mostly interests matrix due to its weakness, starts only when fibers locally change their direction due to the pin movement.

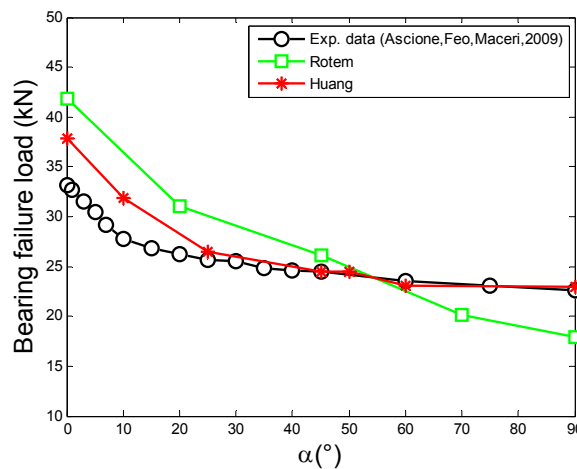


Figure 4: Comparison of predicted failure load with experimental data.

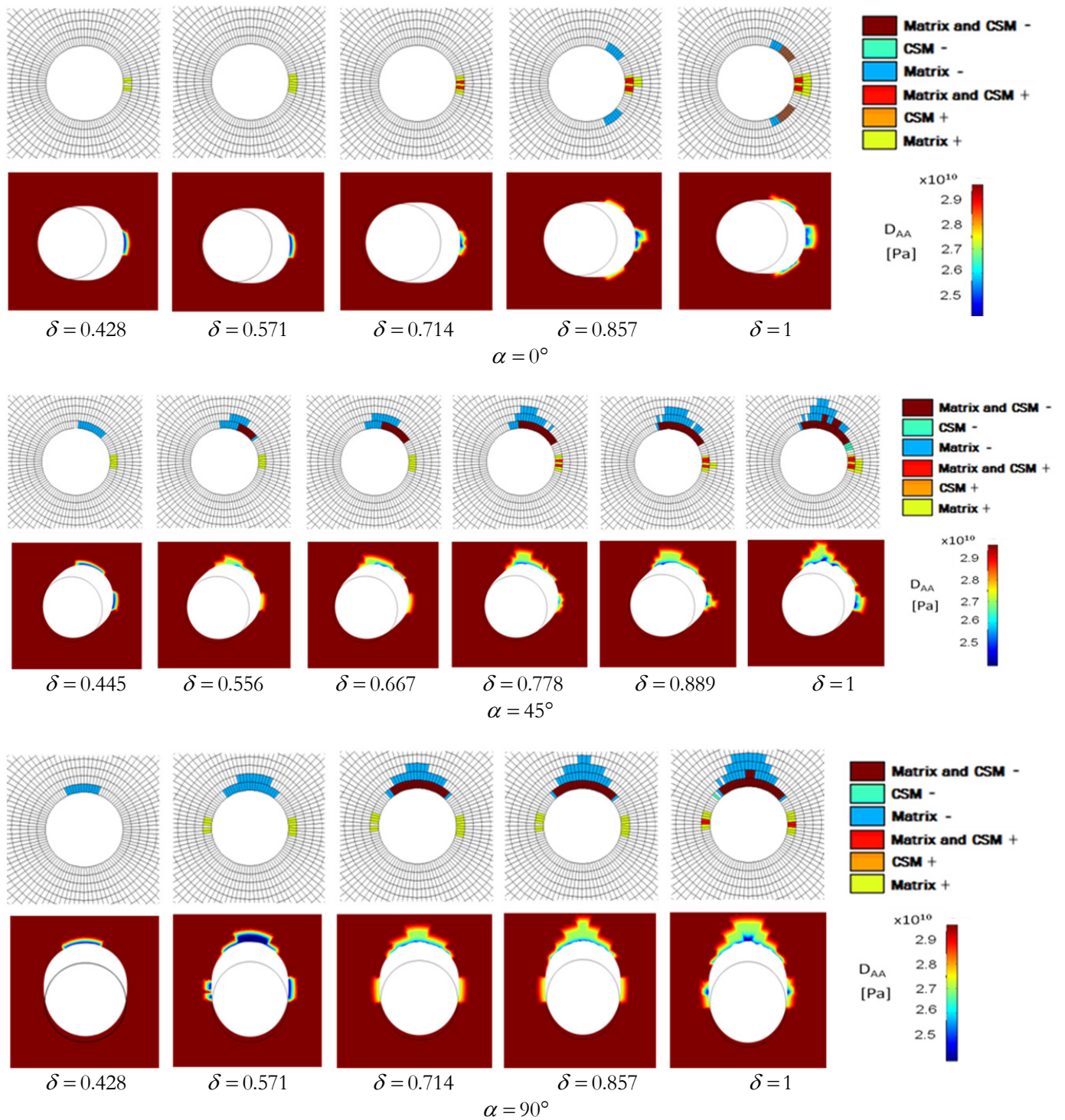


Figure 5: Progressive damage in the composite laminated plate for $\alpha = 0^\circ$, 45° , 90° and for different values of $\delta = u / u_{max}$, where u is current pin displacement and u_{max} is the pin displacement inducing the bearing failure. Moreover, D_{AA} denotes the equivalent material stiffness of the laminate along the fiber direction.

On the other hand, when the pin displacement occurs along the direction orthogonal to the fibers, the Rotem's criterion predicts a damage onset at lower loads than the experiments, since the highest stresses arise in the transverse-to-fiber direction and are entirely associated to the transverse laminate strength ($S_T^{+/-}$, S_{AT}).



As already observed, the Huang's failure criteria gives more accurate results. As long as one of the constituents attains its ultimate stress state, the lamina is considered to fail and its contribution to the overall stiffness matrix of the laminate is reduced. When this micromechanical approach is considered for the evaluation of the failure load, the progressive failure process in the laminate can be more properly understood, and the corresponding failure mode can be straight identified. Therefore, the evaluation of localized stress distributions occurring in the composite constituents seems to be extremely important for predicting the onset of damage mechanisms in the laminated plate. Accordingly, a refined method accounting for localization mechanisms in matrix and fibers, as the one proposed by Huang [14], should be preferred if the aim is the prediction and the analysis of the progressive damaging occurring in bolted FRP joints.

Addressing the Huang's criterion, Fig. 5 shows, for different values of α , the evolution of the failure mechanisms within the plate, from the damage onset up to the global failure. Proposed results, obtained by a post-processing procedure that involves a slave partition with respect to the finite-element mesh, highlight that damage occurs, as expected, close to the contact zone. In this figure, the spatial distributions of the equivalent material stiffness for the laminate along the fiber direction (denoted as D_{AA}) are also provided at different damage levels, aiming to show the damage evolution in terms of material degradation (namely, in the figure blue color indicates the lowest value of the equivalent material stiffness and thereby the damaged region). It is worth pointing out that the proposed model allows to discriminate the constituent within each layer experiencing damage. In the analyzed cases, since the plane stress assumption and the mono-directional plying pattern, damage initiation occurs simultaneously in each FRP layer, or in the CSM layers, or in both. Moreover, the numerical simulations predict a main occurrence of the bearing failure in matrix, in agreement with the experimental results discussed in [10]. Finally, it is worth noting also that the procedure is able to predict the onset of different damage mechanisms, as experienced for $\alpha = 90^\circ$, where a tensile matrix failure is shown in the direction orthogonal to the pin displacement, suggesting the onset of a net-tension failure mechanism together with the bearing one.

CONCLUSIONS

In this paper, a progressive damage model based on a finite-element incremental approach has been proposed, in order to simulate failure mechanisms occurring in bolted joints between fiber-reinforced composite elements. Two available failure criteria (namely, by Rotem and Huang, and differently accounting for micro-structural material features) are employed, and unilateral frictionless contact conditions at the pin-plate interface are included.

The model has been applied to study a pin-plate system. Proposed numerical results predict a bearing failure mechanism fully in agreement with the experimental evidence discussed in [10]. Results in terms of the failure load can be successfully compared with experimental data in a quantitative way only when localization mechanisms in matrix and fibers are suitably accounted for within the formulation of the failure criterion, such as in the Huang's criterion. Nevertheless, some significant discrepancies among numerical results and experiments can be highlighted for small values of the angle between the fiber direction and the load one. In order to overcome such a drawback, and as a perspective application, future works will address the development of an *ad hoc* failure criterion.

Proposed approach opens towards the possibility of simulating progressive damage mechanisms occurring in bolted joints between fiber-reinforced composite structural elements, allowing to provide useful contributions towards the definition of guidelines for design and analysis of FRP bolted joints.

ACKNOWLEDGEMENT

This work was partially supported by the Italian Civil Protection Department [RELUIS-DPC 2014-18, CUP: E84G14000480007] and it was developed within the framework of the Lagrange Laboratory, a European research group comprising CNRS, CNR, the Universities of Rome "Tor Vergata", Calabria, Cassino, Pavia and Salerno, Ecole Polytechnique, University of Montpellier II, ENPC, LCPC and ENTPE.

REFERENCES

- [1] Kelly, G., Hallström, S., Pin-bearing strength of carbon fibre/epoxy laminates: effects of bolt-hole clearance, *Composites Part B: Engineering*, 35 (2004) 331–343.



- [2] Counts, W.A., Johnson, W.S., Bolt pin-bearing fatigue of polymer matrix composites at elevated temperature, *International Journal of Fatigue*, 24 (2002) 197–204.
- [3] Xiao, Y., Ishikawa, T., Bearing strength and failure behaviour of bolted composite joints (part I: experimental investigation), *Composites Science and Technology: Engineering*, 65 (2005) 1022–1031.
- [4] Xiao, Y., Ishikawa, T., Bearing strength and failure behaviour of bolted composite joints (part II: modelling and simulation), *Composites Science and Technology: Engineering*, 65 (2005) 1032–1043.
- [5] Vangrimde, B., Boukhili, R., Pin-bearing stiffness of glass fibre-reinforced polyester: influence of coupon geometry and laminate properties, *Composites Structures*, 58 (2002) 57–73.
- [6] Vangrimde, B., Boukhili, R., Descriptive relationships between pin-bearing response and macroscopic damage in GFRP bolted joints, *Composites Part B: Engineering*, 34(8) (2003) 593–605.
- [7] Vangrimde, B., Boukhili, R., Analysis of the pin-bearing response test for polymer matrix composite laminates: pin-bearing stiffness measurements and simulation, *Composite Structures*, 56 (2002) 359–374.
- [8] Li, R., Kelly, D., Crosky, A., Strength improvement by fibre steering around a pin loaded hole, *Composite Structures*, 57 (2002) 337–383.
- [9] Ascione, F., Feo, L., Maceri, F., An experimental investigation on the pin-bearing failure load of glass fibre/epoxy laminates, *Composites Part B: Engineering*, 40 (2009) 197–205.
- [10] Ascione, F., Feo, L., Maceri, F., On the pin-bearing failure load of GFRP bolted laminates: An experimental analysis on the influence of bolt diameter, *Composites Part B*, 41 (2010) 482–490.
- [11] Barbero, E.J., *Introduction to composite materials design*, Taylor & Francis (1998).
- [12] Kollar, L.P., Springer, G.S., *Mechanics of Composite Structures*, Cambridge University Press (2009).
- [13] Rotem, A., Prediction of laminate failure with the Rotem failure criterion, *Composites Science and Technology*, 58 (1998) 1083–1094.
- [14] Huang, Z.M., A bridging model prediction of the ultimate strength of composite laminates subjected to biaxial loads, *Composites Science and Technology*, 64 (2004) 395–448.
- [15] Huang, Z.M., A unified micromechanical model for the mechanical properties of two constituent composite materials, part V: laminate strength, *Journal of Thermoplastic Composite Materials*, 13 (2000) 190–206.
- [16] Grote, K.H., Antonsson, E.K., *Springer Handbook of Mechanical Engineering*, Springer-Verlag (2009).
- [17] Campbell, F.C., *Structural Composite Materials*, ASM International (2010).